

Topical Review

Non-Stokesian Nature of Transverse Diffusion Within Human Red Cell Membranes

William R. Lieb[†] and Wilfred D. Stein[‡]

[†] Biophysics Section, Blackett Laboratory, Imperial College of Science and Technology, London SW7 2BZ, United Kingdom, and

[‡] Department of Biological Chemistry, Institute of Life Sciences, The Hebrew University, Jerusalem 91904, Israel

Introduction

Although much research has recently been carried out on lateral diffusion in biological membranes (*see* ref. 35 for a recent review), far less attention has been given to the problem of transverse diffusion—diffusion perpendicular to the plane of the membrane. Yet transverse diffusion is of paramount importance not only for understanding the dynamic properties of lipids in membranes but also for predicting the permeabilities of both single cells and epithelia (e.g., kidney, gut, skin and the blood-brain barrier) to physiologically and pharmacologically active agents.

Nature of the Permeability Data

In order to be able to calculate transverse diffusion coefficients from steady-state permeability measurements, it is necessary [29–32] to have accurate values of *basal* permeability coefficients for non-electrolytes, determined under conditions where transport via specific pathways does not occur. Establishing reliable basal permeability values thus requires both the use of accurate experimental methods and an appreciation of the nature of the specific pathways. This latter problem is especially acute with human red cell membranes, which are now known [32] to possess specific transport systems for many small uncharged molecules which had previously been thought [40] to permeate through aqueous pores.

When we last considered the problem of transverse diffusion in biological membranes [30, 31],

very little reliable basal permeability data existed for animal cell membranes, and the conclusions we drew were based largely on much earlier studies with plant cells. Fortunately, this situation has very recently changed: in the last few years, five new studies [4–6, 28, 34] have appeared which, when combined with earlier studies [7, 45], provide for the first time a reasonable number of accurate basal permeability coefficients for a single animal cell membrane—that of the human red blood cell (*see* the Table).

We proceed to discuss these permeability data. Brahm [4] measured the diffusional permeability of human red cells to water in the presence of a large number of chemicals known to inhibit specific transport systems in the red cell. The maximum inhibition was achieved in the presence of *p*-chloromercuribenzoate, when the permeability coefficient fell to $P = 0.0012 \text{ cm sec}^{-1}$ at 25°C. Although it is possible that even this low value represents some contribution from specific pathways [12], such an effect would seem to be small. This is because the residual diffusional permeability in the presence of organic mercurials has the benchmarks of a basal process: a high temperature coefficient ($E_{act} = 60 \text{ kJ mol}^{-1}$) and a low value which is, moreover, equal to that of the residual osmotic permeability [15, 33]. (For the osmotic permeability of lecithin/cholesterol black lipid films, $E_{act} = 55$ to 61 kJ mol^{-1} [38, 39] and $P = 0.0014$ to $0.0030 \text{ cm sec}^{-1}$ at 25°C [13, 15, 38, 39].)

Brahm [5] also measured the values listed for the *n*-alcohols in the Table. Butanol moved too fast to be accurately measured, but the exchange rates of the other alcohols were at least three times slower and thus permeabilities could be estimated reliably after correction for unstirred layers. (Very similar values for all the alcohols listed here were obtained for the dog red cell by independent work-

Table. Experimental parameters for human red cell permeants

Permeant	Basal P (cm sec^{-1})	Volume V ($\text{cm}^3 \text{mol}^{-1}$)	Partition coefficients between solvent and water			
			K-hexadecane	K-oil	K-octanol	K-lipid
1. Water	1.2×10^{-3} [4]	10.6	4.2×10^{-5} [36]	1.3×10^{-3} [27]	0.041	—
2. Methanol	3.7×10^{-3} [5]	21.7	3.8×10^{-3} [17]	9.5×10^{-3} [27]	0.18	0.21
3. Ethanol	2.1×10^{-3} [5]	31.9	5.7×10^{-3} [17]	3.6×10^{-2} [27]	0.48	0.44
4. Urea	7.7×10^{-7} [6]	32.6	2.8×10^{-7}	1.5×10^{-4} [9]	0.0022	0.23
5. Ethanediol	2.9×10^{-5} [28]	36.5	1.7×10^{-5} [36]	4.9×10^{-4} [27]	0.012	0.12
6. Thiourea	1.1×10^{-6} [34]	39.5	—	1.2×10^{-3} [9]	0.072	—
7. <i>n</i> -Propanol	6.5×10^{-3} [5]	42.2	3.3×10^{-2} [17]	1.4×10^{-1} [27]	2.2	1.3
8. Glycerol	1.6×10^{-7} [7]	51.4	2.0×10^{-6} [36]	7.0×10^{-5} [27]	0.0028	0.050
9. Erythritol	6.7×10^{-9} [45]	66.2	—	3.0×10^{-5} [9]	0.0012	0.026
10. <i>n</i> -Hexanol	8.7×10^{-3} [5]	72.9	1.3 [2]	7.6 [27]	110	—

Permeants are numbered in order of increasing molecular volume. All values are at approximately room temperature; where possible, values at 25°C are listed. Numbers in square brackets refer to data sources. P is the basal permeability coefficient for the human red cell membrane, corrected where appropriate by the investigators for the presence of unstirred layers. V is the van der Waals volume, calculated using the procedures in ref. 3. Partition coefficients K are expressed in volume units. The *K-hexadecane* value for urea was determined by A. Walter and J. Gutknecht (*personal communication*). *K-octanol* values are from ref. 27, and *K-lipid* values are from ref. 25. Additional comments on these data are given in the text and in ref. 32.

ers [19] using a completely different technique.) Since the alcohol movements [5] showed no saturation, had high temperature coefficients, and were not inhibited by *p*-chloromercuribenzenesulfonate or phloretin, it is reasonable to consider the listed values to be basal values.

Urea transport [6] in human red cells is inhibited competitively by urea analogues and noncompetitively by phloretin and *p*-chloromercuribenzenesulfonate, and the maximum inhibition left a ground permeability of $7.7 \times 10^{-7} \text{ cm sec}^{-1}$, which we have taken as the basal permeability to urea. Mayrand and Levitt [34] found that thiourea is transported via both saturable and nonsaturable pathways, and the nonsaturable pathway (which was not affected by the competitive analogue urea) had a basal $P = 1.1 \times 10^{-6} \text{ cm sec}^{-1}$. The values listed for ethanediol [28] and glycerol [7] were obtained in the presence of copper ions, which are known to inhibit specific glycol transport systems. Finally, the value for erythritol (which can enter red cells via the glucose system) was measured by Wieth [45] as the hexose-insensitive permeability, which he found to be unaffected by phloretin and copper ions.

Dependence of Basal Permeability on Solubility

In Fig. 1A we have plotted, on log-log scales, these basal permeability coefficients P against their corresponding *n*-hexadecane/water partition coefficients. We have chosen hexadecane here for two reasons: First, as Finkelstein [16] has stressed, hexadecane is a reasonable *a priori* model for the

solubility properties of the hydrocarbon interior of the membrane. Secondly, as we will show later, although hexadecane is an extremely poor model for the diffusional behavior of the rate-limiting barrier for basal permeation, it is a good model for the solubility characteristics of this barrier.

What is surprising about Fig. 1A is that the data points deviate so markedly from the least squares straight line of unit slope. This is contrary to the rule of Overton [37], which predicts that all points should lie along this line. Overton's rule is based on the implicit premise that diffusion rates within the membrane, as in a simple liquid like water, do not vary much from permeant to permeant, so that the major factor discriminating between different permeants is their solubility. What is the reason for this breakdown in Overton's rule?

Dependence of Basal Permeability and Transverse Diffusion on Permeant Volume

A closer inspection of Fig. 1A reveals an important clue: those permeants which lie above the regression line of unit slope have low molecular volumes whereas those which lie furthest below the line have the highest molecular volumes. This immediately suggests that, solubilities in the membrane interior being equal, large permeant molecules find it much more difficult to cross the human red cell membrane than do small molecules.

This result can be placed on a quantitative basis—and one which has the attraction of providing a molecular interpretation—by considering the sim-

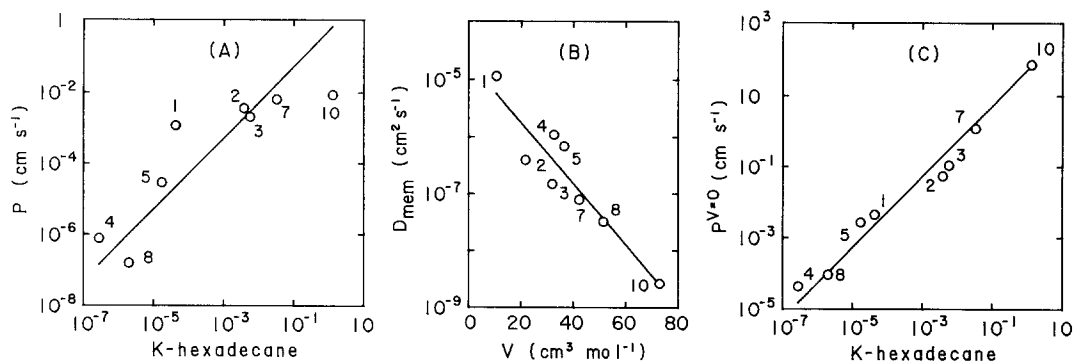


Fig. 1. Departures from Overton's rule can be accounted for by a steep volume dependence of transverse membrane diffusion. (A) Poor fit of human red cell basal permeability coefficients P to Overton's rule. The straight line is the least squares line of unit slope. (B) Steep volume dependence of transverse diffusion within the membrane. The transverse diffusion coefficient D_{mem} is plotted against the van der Waals volume V on semilogarithmic scales. The slope (\pm SE) of the least squares line is $-0.054 (\pm 0.008) \text{ mol cm}^{-3}$. (C) Good fit of volume-corrected basal permeability coefficients $P^{V=0}$ to Overton's rule. The straight line is the least squares line of unit slope. Values of P and n -hexadecane/water partition coefficients K -hexadecane are listed in the Table. D_{mem} values were calculated using Eq. (2) with $d_{\text{mem}} = 40 \text{ \AA}$ and $K_{\text{mem}} = K$ -hexadecane. $P^{V=0}$ values were then calculated using Eq. (4) with $m_v = 0.054 \text{ mol cm}^{-3}$ [from the slope of (B)] and van der Waals volumes V from the Table. Notice that permeants are numbered in order of increasing volumes (see Table)

plest of all models for nonspecific permeation: the rate-limiting barrier for permeation is a region of thickness d_{mem} with an average partition coefficient K_{mem} and transverse diffusion coefficient D_{mem} for a given permeant molecule. For such a solubility/diffusion model, the overall basal permeability coefficient P is given by [11, 29]

$$P = K_{\text{mem}} D_{\text{mem}} / d_{\text{mem}}. \quad (1)$$

Thus transverse diffusion coefficients can be obtained [22, 29–32] using

$$D_{\text{mem}} = P d_{\text{mem}} / K_{\text{mem}}. \quad (2)$$

In practice, of course, we know neither d_{mem} nor K_{mem} , since the rate-limiting barrier within the membrane is unknown. However, since d_{mem} will be roughly the same for a set of similar molecules, it is not important what value we use for it; we will take $d_{\text{mem}} = 40 \text{ \AA}$ (the approximate thickness of the hydrocarbon region of most biological membranes) as a reasonable estimate. The choice of estimates for K_{mem} is more problematical. For present purposes, we will assume (as above) that K -hexadecane values provide reasonable estimates. Later, we will show that the conclusions to be reached about the nature of the transverse diffusion process are insensitive to the choice of the model solvent.

The transverse diffusion coefficients D_{mem} so calculated are plotted, on semilogarithmic scales, against permeant volumes in Fig. 1B. (We use van der Waals volumes rather than the more commonly used molar volumes, both in order to have volume

estimates that are not biased by intermolecular forces which may only be present in the pure chemical and also because they are more appropriate for the quantitative theory of diffusion, which we shall develop later. This theory predicts a straight line if data are plotted as in Fig. 1B.) Clearly, D_{mem} depends very steeply upon V . The slope (\pm SE) of the straight line in Fig. 1B is $-0.054 (\pm 0.008) \text{ mol cm}^{-3}$. This means, for example, that doubling the volume of a permeant whose size is similar to that of ethanol ($V = 32 \text{ cm}^3 \text{ mol}^{-1}$) decreases D_{mem} , on average, by the factor $10^{0.054(32)} \approx 50$. The corresponding factor for diffusion in a simple Stokesian liquid (see below) is only about $2^{1/3} = 1.3$. Thus it appears that transverse diffusion across the human red cell membrane is enormously more sensitive to permeant volume than is diffusion in simple liquids. Similarly large dependences of diffusion upon diffusant volume are seen for diffusion in other structured media, e.g. polymers [29–32], and we will discuss the possible molecular reasons for this later.

Dependence of Basal Permeability on Both Solubility and Volume

If the departures from Overton's rule we saw in Fig. 1A are indeed due to an anomalously steep volume dependence of transverse diffusion within the interior of the human red cell membrane, then the data should conform to Overton's rule once this has been taken into account. What we need are size-corrected permeability coefficients, corrected for the volume dependence of the diffusion step.

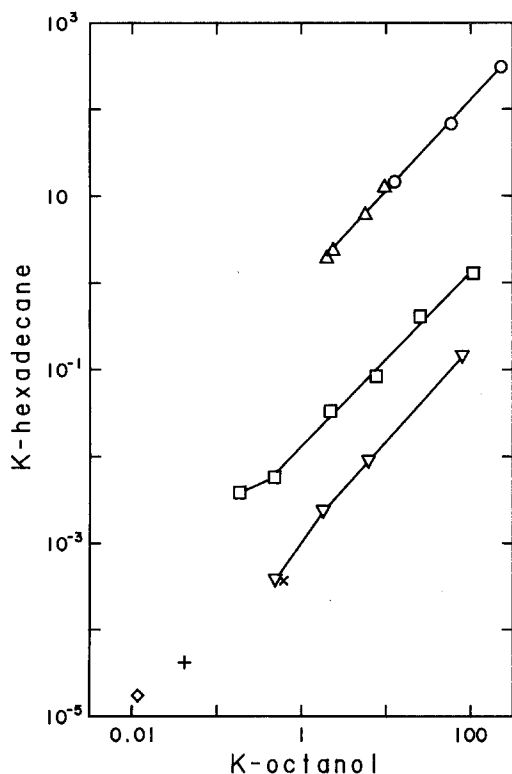


Fig. 2. The relationship between *n*-hexadecane/water and *n*-octanol/water partition coefficients for different classes of compounds. To avoid any theoretical bias, only directly measured partition coefficients (from refs. 32 and 43) have been plotted. The symbols are: Δ , rare gases; \circ , *n*-alkanes; \square , *n*-alcohols; ∇ , *n*-carboxylic acids (neutral form); \times , *n*-butylamide; $+$, water \diamond , ethanediol

We note that the straight line in Fig. 1B obeys the equation

$$D_{\text{mem}} = D_{\text{mem}}^{V=0} 10^{-(m_v V)} \quad (3)$$

where m_v , the negative of the slope, is a measure of the volume selectivity of the transverse diffusion process and $D_{\text{mem}}^{V=0}$, the intercept on the ordinate axis, is the limitingly high transverse diffusion coefficient (for a theoretical molecule of vanishingly small volume). Using Eqs. (1) and (3), we obtain a size-corrected permeability coefficient:

$$P^{V=0} \equiv K_{\text{mem}} D_{\text{mem}}^{V=0} / d_{\text{mem}} = P 10^{(m_v V)}. \quad (4)$$

Figure 1C is a plot of these size-corrected basal permeability coefficients against *K*-hexadecane. This plot is, of course, merely a transformation of the plot of Fig. 1B, but it enables one to look at the data from the perspective of Overton's rule. In contrast to the uncorrected plot (Fig. 1A), the fit of the data to the least squares line of unit slope is now very good. Equally important, a closer inspection of

Fig. 1C shows that there is no longer any systematic size-dependent deviation of points from this line. Thus the departures from Overton's rule in Fig. 1A can be very largely accounted for by the hypothesis that there is a very steep volume dependence in the transverse diffusion step.

Analysis of Permeability Data for Other Membranes

Many permeability studies are inadequate for the present type of analysis, for any of the following reasons: (1) It is not at all clear if the permeabilities being measured are basal rather than specific. (2) Unstirred layers are not adequately taken into account. (3) Permeant concentrations are often so high that the membranes are probably fluidized.

Fortunately, many published studies do not appear to have these problems, and we have analyzed them in detail in ref. 32. Results similar to those of Fig. 1 were observed for both biological membranes (animal and plant) and lipid bilayers (liposomes and black films). (The only exceptions to a steep volume dependence which we have found were some studies [26, 43] on the permeabilities of homologous series of fatty acids performed under conditions when most of the acids were in their dissociated charged forms; the reason for this discrepancy is not yet clear.) Thus a steep volume dependence of transverse diffusion would seem to be a common feature of most biological and lipid membranes.

In general, the size dependence of the diffusion step appears to be somewhat greater for biological than for pure lipid membranes [32]. This may reflect the presence of more constraints on lipid motion in biological membranes than in protein-free lipid bilayers. The differing basal permeability properties of different biological and lipid membranes are probably largely due to such constraints, which will vary with the type of lipids (cholesterol being particularly important) and proteins present in the membranes.

Choice of a Model Solvent

It is often said that the choice of a model solvent for the partitioning behavior of the major transport barrier is a phantom problem because partition coefficients in different solvents are related to each other by constant ratios. That this is not true can be seen from Fig. 2, where we have plotted, on log-log scales, directly measured values of *K*-hexadecane and *K*-octanol for different classes of compounds. The uppermost line is for apolar compounds (rare

gases and lower alkanes), the middle line for alcohols, and the lowest line for carboxylic acids. (Single data points are included for an amide, water and a vicinal diol.) Each successive line thus represents families of compounds having progressively larger numbers of hydrogen-bonding functions (none, hydroxyl and carboxyl, respectively). If we were to compare any two solvents which differ in their partitioning behavior, we would presumably get a plot similar to that in Fig. 2, with the corresponding lines being more spread out or less so, depending on whether the two solvents differ more or less. Only if two solvents have the same partitioning behavior will the lines coalesce to a single common line.

This forms the basis of a protocol for choosing the best model solvent for the partitioning behavior of an unknown site. For an equilibrium phenomenon, the procedure is simple. For example, Franks and Lieb [17] plotted, on log-log scales, general anesthetic potencies for animals versus *K-hexadecane*, *K-oil* and *K-octanol* and found that the data points coalesced onto a single common line only with *K-octanol*. From this they concluded that *n*-octanol best reflected the solubility characteristics of the unknown target sites in general anesthesia, presumably because these sites are amphiphilic in nature.

Permeability, on the other hand, is a rate phenomenon which contains contributions from both an equilibrium step (partitioning) and a nonequilibrium step (transverse diffusion). If we could somehow separate out the partitioning step from the diffusion step, then we could proceed as above. Fortunately, the size-corrected permeability coefficient, $P^{V=0}$, introduced earlier enables us to do precisely this since, as can be seen from the defining Eq. (4), $P^{V=0}$ is directly proportional to K_{mem} .

Figure 3 shows the use of the protocol for the human red cell data of the Table, using four different partitioning systems of increasing hydrophobicity: (A) lipid bilayers, (B) *n*-octanol, (C) vegetable oil and (D) *n*-hexadecane. The different symbols distinguish permeants having different degrees of hydrogen-bonding capacity; the "heavier" the symbol the greater is the hydrogen-bonding capacity. The lines are the least squares lines of unit slope. [Notice from the legend the very important result that large volume selectivities for transverse diffusion are found for all four partitioning systems, so that this finding (see Fig. 1B) is independent of the choice of partitioning system.]

Clearly lipid bilayers are a poor choice, since the data points in Fig. 3A are widely scattered and lie far from the line of unit slope. In Fig. 3B for octanol, the data points for the permeants of lowest hydrogen-bonding capacity (the homologous series

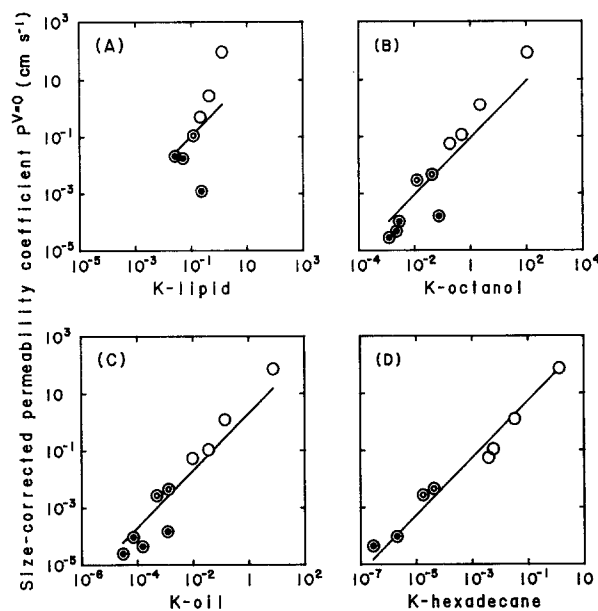


Fig. 3. Size-corrected basal permeability coefficients $P^{V=0}$ for the human blood red cell plotted against partition coefficients in four systems, in order of increasing hydrophobicity: (A) lipid bilayers, (B) *n*-octanol, (C) vegetable oil and (D) *n*-hexadecane. The straight lines are the least squares lines of unit slope. For each system, values of the volume selectivity parameter m_v were first determined as in Fig. 1B by plotting $\log_{10}(D_{\text{mem}})$ against V ; the resulting values of m_v were (A) 0.0982, (B) 0.0546, (C) 0.0538 and (D) 0.0539 mol cm^{-3} . Using these values of m_v and values of P and V from the Table, values of $P^{V=0} = P10^{(m_v, V)}$ were calculated and are plotted above using the K values listed in the Table. Permeants are grouped according to their relative hydrogen-bonding capacities: empty circles, weak hydrogen-bonders (*n*-alcohols); empty concentric circles, moderate hydrogen-bonders (water, ethanediol); filled concentric circles, strong hydrogen-bonders (urea, thiourea, glycerol, erythritol)

of *n*-alcohols) define, more or less, a line lying above the regression line of unit slope, whereas data points for those permeants of greatest hydrogen-bonding capacity all lie below this line. This is very reminiscent of Fig. 2, where we plotted partition coefficients for a very hydrophobic solvent (hexadecane) against those for a less hydrophobic solvent (octanol), and it suggests that the red cell permeability barrier is more hydrophobic than octanol. Indeed, it can be seen from Fig. 3C that the more hydrophobic solvent olive oil *does* bring the data points closer to the common line, but the stronger hydrogen-bonders still lie below, and the weaker above, the line of unit slope. Only with the very apolar solvent hexadecane (Fig. 3D) do we approach a more or less equal distribution of strong and weak hydrogen-bonding permeants. There is even a hint that the pattern for *n*-hexadecane is the reverse of that for the other systems, in that the

weaker hydrogen-bonders tend to lie below, and the stronger above, the common line in Fig. 3D. Unfortunately, however, for *n*-hexadecane we lack the partitioning data which might resolve this issue: data for two of the strongest hydrogen-bonders (thiourea and erythritol). It may be that the best model would be a solvent slightly more polar than *n*-hexadecane, perhaps, in view of the hydrocarbon chain composition of the red cell membrane, an unsaturated long-chain hydrocarbon.

Thus the analysis of Fig. 3 indicates that the major barrier for the nonspecific permeation of simple uncharged molecules across the human red cell membrane is very hydrophobic (apolar). This is consistent with it being in the hydrocarbon interior of the lipid bilayer portion of the membrane (but inconsistent with our previous suggestion [46] that the barrier is at the glycerol backbone region of the bilayer!). Notice that a naive use of partition coefficients between lipid bilayers and water would have been completely unjustified—see Fig. 3A. This is because most of these hydrophilic or amphiphilic permeant molecules are concentrated near the bilayer/water interfaces [10] and not in the hydrocarbon interior. It is not possible from our analysis to say where in the hydrocarbon interior the barrier lies. However, it seems most likely that it is the tightly packed regions [18] containing the cholesterol steroid nuclei (red cell membranes contain high concentrations of cholesterol) rather than the more flexible hydrocarbon tail region at the bilayer center.

It is, of course, not presently possible to actually measure the partitioning behavior of this major permeability barrier, both because its exact location is unknown and because the permeant molecules we have been considering are only sparingly soluble in the hydrocarbon interior of the membrane. However, some very interesting experimental [1, 14, 23, 44] and statistical thermodynamic [20, 21] studies on the uptake of apolar *n*-alkanes by black lipid films show a cut-off size beyond which large alkanes are adsorbed into the bilayer interior less than expected from the behavior of small alkanes. For egg lecithin films the deviant behavior begins only after *n*-decane, but replacement of about 30% (on a mole basis) of the lecithin with cholesterol causes alkanes as small as *n*-octane to become deviant [23]. For red cell membranes, which contain not only more cholesterol but also protein, the cut-off size could be even smaller. If so, this could contribute to the observed size dependency of permeation, and one must therefore be cautious in attributing all of this to diffusion. However, for the permeants considered in our analysis, the derived values of $\log(D_{\text{mem}})$ decrease linearly from water to hexanol

(see Fig. 1B) with no apparent cut-off. We therefore suspect that such size-dependent partitioning plays only a minor role in our present analysis, but it might well play a major role for permeants larger than those considered here.

Molecular Basis of the Steep Size Dependence of Transverse Diffusion: Non-Stokesian Diffusion

For a sphere of radius *r* diffusing in a continuous fluid, the diffusion coefficient *D* is given by the well-known Stokes-Einstein equation:

$$D = kT/(6\pi\eta r) \quad (5)$$

where *k* is the Boltzmann constant, *T* is the absolute temperature, and η is the coefficient of viscosity. The denominator, $6\pi\eta r$, is the factor which G.G. Stokes found necessary to describe the frictional drag on a sphere moving through a viscous fluid. Stokes' factor can be derived from standard fluid-dynamic considerations [41]: the diffusing particle carries with it a shell of fluid which is at rest with respect to the particle itself, and there is a gradient of velocities between this immobilized shell and the bulk fluid. (There is an analogy here with the more familiar Poiseuillian flow of a fluid through a cylindrical tube, where the walls of the tube bear an immobilized layer of fluid and there is a gradient of velocities towards the center of the tube.) It is the frictional drag between layers of fluid which determines the frictional resistance to diffusion, and this resistance increases relatively slowly as the size of the diffusing particles increases: for spheres, this resistance increases only as the cube root of the volume. We shall call this type of fluid-dynamic movement *Stokesian* diffusion.

In contrast, the type of diffusion we have seen for transverse movement across membranes decreases in value steeply with permeant size (see, for example, Fig. 1B) and hence does not obey the Stokes-Einstein equation. Thus for transverse movement within biological membranes we are dealing with *non-Stokesian* diffusion.

What is the molecular basis of this type of non-Stokesian diffusion? Some clues come from a consideration of the properties of diffusion in other media. For example, diffusion within soft polymer networks often displays steep volume dependencies [29–32]. On the contrary, diffusion within liquids does not: diffusion in liquid *n*-hexadecane and in water displays the weak type of volume dependence inherent in the Stokes-Einstein equation [24, 31–32]. (This means that hexadecane, although an excellent model for the partitioning behavior of the

rate-limiting barrier for basal permeation in red cell membranes, is a very poor model for the diffusional behavior of this barrier.) What seems to differentiate these two types of diffusional behavior is the ability (Stokesian) or the inability (non-Stokesian) of molecules of the diffusing medium to flow around the diffusing molecule. This inability to flow around a diffusing molecule is almost certainly true for a nonfluid polymer network such as rubber, but is it also true for the lipid bilayer portions of biological membranes? For the *lateral* diffusion of small molecules in these membranes, the answer is probably "no," since lipid molecules are very mobile in the plane of the membrane. However, for *transverse* diffusion, in the direction normal to this plane, the answer appears to be "yes." This may be because the lipids and their hydrocarbon chains are anchored to the membrane/water interfaces and thus cannot easily flow past the diffusant molecules.

If in non-Stokesian diffusion the molecules of the diffusing media cannot flow around the diffusing molecule, then, before it can move, it must await the formation of a suitably sized packet of free volume, or "hole," adjacent to it [31]. (Trauble [42] has emphasized the possible importance of hydrocarbon chain "kinks" in the formation of such holes in his "mobile kink" theory, which is a special case of the treatment which follows.) When this happens, the molecule can then move by jumping into the hole. Since a suitably sized hole must have a volume greater than or equal to the volume of the diffusant molecule, and since there will always be more small holes than large holes (*see* below), it follows that small molecules will diffuse much more rapidly than large molecules. (Since holes are also present in simple liquids, presumably such hole-jumping pathways are also available for diffusion there but are quantitatively much less important than the fluid-dynamic pathways.)

In order to put these ideas concerning non-Stokesian diffusion into a semi-quantitative framework, consider the following approach (simplified from ref. 32). For a non-Stokesian medium at a fixed temperature, the diffusion coefficient D should, to a first approximation, be proportional to the probability $f(V)$ that a given hole has a volume equal to or larger than the volume V of the diffusing molecule. The very simplest statistical mechanical model for hole size distribution in liquids suggests that the probability $P(V)dV$ of finding a hole whose volume lies between V and $V + dV$ is given by

$$P(V)dV = (1/\bar{V}) \exp(-V/\bar{V})dV \quad (6)$$

where \bar{V} is the mean volume of a hole [8]. The probability $f(V)$ of a hole having a volume greater

than or equal to V can then be found by integrating Eq. (6) between V and infinity, which gives

$$f(V) = \exp(-V/\bar{V}). \quad (7)$$

Thus we have the result that the overall diffusion coefficient is given by

$$D = (\text{constant}) \exp(-V/\bar{V}). \quad (8)$$

Now what is interesting is that Eq. (8) is equivalent in form to Eq. (3) for transverse diffusion within the human red cell membrane, which can be rewritten in the form:

$$D_{\text{mem}} = D_{\text{mem}}^{V=0} \exp(-2.3 m_v V). \quad (9)$$

A comparison of Eqs. (8) and (9) shows that, on this simple model, the average free volume $\bar{V} = (2.3 m_v)^{-1}$. Substituting the value of $m_v = 0.054 \text{ mol cm}^{-3}$ found earlier (Fig. 1B), it follows that the mean hole size within that portion of the hydrocarbon interior of the red cell membrane which forms the major barrier to diffusion is $\bar{V} = 8 \text{ cm}^3 \text{ mol}^{-1}$, which is slightly less than the van der Waals volume ($10 \text{ cm}^3 \text{ mol}^{-1}$) of a methylene group on a lipid hydrocarbon chain [3]. Thus there is a reasonable quantitative basis for the steep size selectivity found for transverse diffusion within biological membranes.

In summary, we have analyzed recently obtained data on the nonspecific permeation of uncharged molecules across the human red blood cell membrane in terms of solubility/diffusion mechanism. We have introduced a new protocol for selecting that model solvent that best accounts for the solubility properties of the major barrier to permeation. Application of this protocol to the red cell data showed that the best choice is a solvent less polar than octanol or olive oil, approaching the apolarity of *n*-hexadecane. We found that diffusion of nonelectrolyte molecules perpendicular to the plane of the membrane is steeply dependent on diffusant volume. These results can be accounted for quantitatively if transverse diffusion occurs by a hole-jumping (non-Stokesian) rather than a fluid-dynamic (Stokesian) mechanism within the hydrocarbon interiors of biological membranes.

It is a pleasure to acknowledge the helpful comments of our colleagues Felix Bronner, Jared Diamond, Alan Finkelstein, Nick Franks, John Gutknecht, Dennis Haydon, Joseph Hoffman, Dennis Koppel, Mark Milanick, and Arthur Solomon.

References

1. Andrews, D.M., Manev, E.D., Haydon, D.A. 1970. Composition and energy relationships for some thin lipid films, and the chain conformation in monolayers at liquid-liquid interfaces. *Spec. Discuss. Faraday Soc.* **1**:46–56
2. Aveyard, R., Mitchell, R.W. 1969. Distribution of *n*-alkanols between water and *n*-alkanes. *Trans. Faraday Soc.* **65**:2645–2653
3. Bondi, A. 1964. van der Waals volumes and radii. *J. Phys. Chem.* **68**:441–451
4. Brahm, J. 1982. Diffusional water permeability of human erythrocytes and their ghosts. *J. Gen. Physiol.* **79**:791–819
5. Brahm, J. 1983. Permeability of human red cells to a homologous series of aliphatic alcohols. *J. Gen. Physiol.* **81**:283–304
6. Brahm, J. 1983. Urea permeability of human red cells. *J. Gen. Physiol.* **82**:1–23
7. Carlsen, A., Wieth, J.O. 1976. Glycerol transport in human red cells. *Acta Physiol. Scand.* **97**:501–513
8. Cohen, M.H., Turnbull, D. 1959. Molecular transport in liquids and glasses. *J. Chem. Phys.* **31**:1164–1169
9. Collander, R., Bärlund, H. 1933. Permeabilitätsstudien an *Chara ceratophylla*. *Acta Bot. Fenn.* **11**:1–114
10. Diamond, J.M., Katz, Y. 1974. Interpretation of nonelectrolyte partition coefficients between dimyristoyl lecithin and water. *J. Membrane Biol.* **17**:121–154
11. Diamond, J.M., Wright, E.M. 1969. Biological membranes: The physical basis of ion and nonelectrolyte selectivity. *Annu. Rev. Physiol.* **31**:581–646
12. Dix, J.A., Solomon, A.K. 1984. Role of membrane proteins and lipids in water diffusion across red cell membranes. *Biochim. Biophys. Acta* **773**:219–230
13. Fettiplace, R. 1978. The influence of the lipid on the water permeability of artificial membranes. *Biochim. Biophys. Acta* **513**:1–10
14. Fettiplace, R., Andrews, D.M., Haydon, D.A. 1971. The thickness, composition and structure of some lipid bilayers and natural membranes. *J. Membrane Biol.* **5**:277–296
15. Fettiplace, R., Haydon, D.A. 1980. Water permeability of lipid membranes. *Physiol. Rev.* **60**:510–550
16. Finkelstein, A. 1976. Water and nonelectrolyte permeability of lipid bilayer membranes. *J. Gen. Physiol.* **68**:127–135
17. Franks, N.P., Lieb, W.R. 1978. Where do general anaesthetics act? *Nature (London)* **274**:339–342
18. Franks, N.P., Lieb, W.R. 1979. The structure of lipid bilayers and the effects of general anaesthetics: An X-ray and neutron diffraction study. *J. Mol. Biol.* **133**:469–500
19. Garrick, R.A., Patel, B.C., Chinard, F.P. 1980. Permeability of dog erythrocytes to lipophilic molecules: Solubility and volume effects. *Am. J. Physiol.* **238**:C107–C113
20. Gruen, D.W.R. 1981. A mean-field model of the alkane-saturated lipid bilayer above its phase transition: I. Development of the model. *Biophys. J.* **33**:149–166
21. Gruen, D.W.R., Haydon, D.A. 1981. A mean-field model of the alkane-saturated lipid bilayer above its phase transition: II. Results and comparison with experiment. *Biophys. J.* **33**:167–188
22. Hanai, T., Haydon, D.A. 1966. The permeability to water of bimolecular lipid membranes. *J. Theoret. Biol.* **11**:370–382
23. Haydon, D.A., Hendry, B.M., Levinson, S.R., Requena, J. 1977. Anaesthesia by the *n*-alkanes: A comparative study of nerve impulse blockage and the properties of black lipid bilayer membranes. *Biochim. Biophys. Acta* **470**:17–34
24. Hayduk, W., Ioakimidis, S. 1976. Liquid diffusivities in normal paraffin solutions. *J. Chem. Eng. Data* **21**:255–260
25. Katz, Y., Diamond, J.M. 1974. Thermodynamic constants for nonelectrolyte partition between dimyristoyl lecithin and water. *J. Membrane Biol.* **17**:101–120
26. Klocke, R.A., Flasterstein, F. 1982. Kinetics of erythrocyte penetration by aliphatic acids. *J. Appl. Physiol.* **53**:1138–1143
27. Leo, A., Hansch, C., Elkins, D. 1971. Partition coefficients and their uses. *Chem. Rev.* **71**:525–616
28. Levitt, D.G., Mlekoday, H.J. 1983. Reflection coefficient and permeability of urea and ethylene glycol in the human red cell membrane. *J. Gen. Physiol.* **81**:239–253
29. Lieb, W.R., Stein, W.D., 1969. Biological membranes behave as non-porous polymeric sheets with respect to the diffusion of non-electrolytes. *Nature (London)* **224**:240–243
30. Lieb, W.R., Stein, W.D. 1971. Implications of two different types of diffusion for biological membranes. *Nature New Biol.* **234**:220–222
31. Lieb, W.R., Stein, W.D. 1971. The molecular basis of simple diffusion within biological membranes. In: *Current Topics in Membranes and Transport*. Vol. 2; pp. 1–39. F. Bronner & A. Kleinzeller, editors. Academic Press, New York
32. Lieb, W.R., Stein, W.D. 1986. Simple diffusion across the membrane bilayer. In: *Transport and Diffusion across Cell Membranes*. W.D. Stein. pp. 69–112. Academic Press, Orlando
33. Macey, R.I., Karan, D.M., Farmer, R.E.L. 1972. Properties of water channels in human red cells. In: *Biomembranes*. Vol. 3, pp. 331–340. F. Kreuzer and J.F.G. Slegers, editors. Plenum, New York
34. Mayrand, R.R., Levitt, D.G. 1983. Urea and ethylene glycol-facilitated transport systems in the human red cell membrane. *J. Gen. Physiol.* **81**:221–237
35. McCloskey, M., Poo, M-m. 1984. Protein diffusion in cell membranes: Some biological implications. *Int. Rev. Cytol.* **87**:19–81
36. Orbach, E., Finkelstein, A. 1980. The nonelectrolyte permeability of planar lipid bilayer membranes. *J. Gen. Physiol.* **75**:427–436
37. Overton, E. 1895. Über die osmotischen Eigenschaften der lebenden Pflanzen- und Tierzelle. *Vierteljahrssch. Naturforsch. Ges. Zuer.* **40**:159–201
38. Price, H.D., Thompson, T.E. 1969. Properties of liquid bilayer membranes separating two aqueous phases: Temperature dependence of water permeability. *J. Mol. Biol.* **41**:443–457
39. Redwood, W.R., Haydon, D.A. 1969. Influence of temperature and membrane composition on the water permeability of lipid bilayers. *J. Theoret. Biol.* **22**:1–8
40. Solomon, A.K. 1960. Pores in the cell membrane. *Sci. Am.* **203**:146–156
41. Tanford, C. 1961. *Physical Chemistry of Macromolecules*. pp. 324–327. Wiley, New York
42. Träuble, H. 1971. The movement of molecules across lipid membranes: A molecular theory. *J. Membrane Biol.* **4**:193–208

43. Walter, A., Gutknecht, J. 1984. Monocarboxylic acid permeation through lipid bilayer membranes. *J. Membrane Biol.* **77**:255-264
44. White, S.H. 1977. Studies of the physical chemistry of planar bilayer membranes using high-precision measurements of specific capacitance. *Ann. N.Y. Acad. Sci.* **303**:243-265
45. Wieth, J.O. 1971. Effects of hexoses and anions on the erythritol permeability of human red cells. *J. Physiol. (London)* **213**:435-453
46. Wolosin, J.M., Ginsburg, H., Lieb, W.R., Stein, W.D. 1978. Diffusion within egg lecithin bilayers resembles that within soft polymers. *J. Gen. Physiol.* **71**:93-100

Received 23 December 1985; revised 16 April 1986